

Characterization of Nano- Crystalline NiP Alloy Coatings Electrodeposited at Various Current Densities

Lekmine Faride¹, Ben Temam Hachemi², Guettaf Temam Elhachmi^{2,*}

* *elhachemi.guettaf@univ-biskra.dz*

¹Physics laboratory of Thin Layers and Applications, University Abbes Laghrour, Khenchela, Algeria

²Physics laboratory of Thin Layers and Applications, Biskra University, BP 145 RP, Biskra, Algeria

Received: April 2021

Revised: July 2021

Accepted: July 2021

DOI: 10.22068/ijmse.2237

Abstract: Nickel phosphorus alloy coatings were prepared by electrodeposition route from sulfate electrolyte bath at various current densities. SEM studies revealed that spherical grains covered the entire surface with uniform distribution. EDX results showed a linear increase of P content in the developed deposits with current density, causing an increase in the grains size and a drop in hardness values. XRD studies revealed monocrystalline orthorhombic alloys at low phosphorus content (10.88 wt. %). Corrosion test results showed that 1 A.dm⁻² is the best applied current density providing the nobler E_{corr} (-171.4 mV) and the lower i_{corr} (4.64 μ A/cm²).

Keywords: NiP alloy coatings, Crystal structure, P content, Hardness, Electrochemical properties.

1. INTRODUCTION

Numerous researchers are interested in the fabrication of Ni-P alloy coatings by electrochemical methods such as electrodeposition and electroless deposition, from baths containing phosphorous compound and the iron group as based metal matrix [1-4]. Yosuke Suzuki et al [5] reported the several disadvantages of electroless deposition technique, such as a chemically unstable plating bath and a relatively high temperature required to increase deposition speed. While alloy coatings require low cost and high productivity, electrodeposition is the most suitable technique.

Due to their good properties such as corrosion resistance [6], and high hardness [7], Ni-P alloys are good candidates to replace chromium alloys. This latter, with wide applications in electronics, automotive, aircraft, and decorative sectors causes major problems, especially those related to health and environment, due to the presence of hexavalent chromium in the electrolyte [8].

The role of phosphorous has been a subject of interest in view of phase transitions and the physical properties of Ni-P alloys. X-ray diffraction (XRD) is a conventional technique for investigating phases of Ni-P electrodeposits [9]. Several studies on Ni-P alloy coatings have shown that the nickel phase with fcc structure is forming first, then the formation of Ni₃P phase. Also, the crystallization decreases with increased

phosphorus amount [10-12]. Two different mechanisms have been proposed to describe this type of coating [13]. The direct mechanism has been proposed by Brenner [14], and the indirect mechanism suggested by Zellar and Landau [15]. In the light of the first mechanism, Morikawa et al explicitly studied the Ni-P coating in a nickel-citrate bath [16], which has also been extensively studied in terms of its preparation, properties, and structural transitions. Pillai et al, have shown that phosphorus cannot be deposited only with the presence of a metal iron group such as nickel by co-deposition technique [17]. Therefore, the amount of P in the alloy affects its crystallographic structure; increasing of the P content in the deposit changes the microstructure from a crystalline state to a nanocrystalline state and finally to an amorphous state. Moreover, Saitou et al investigated both the indirect and direct mechanisms and found that the electrodeposited Ni-P alloy is to have an amorphous structure similar to rapid-quenched Ni-P alloys, which describe the indirect incorporation of phosphorous [9].

Ni-P coating has been widely used in the electronics industry as a protective barrier between copper and gold against corrosion in microelectronics [18]. Yihui You et al reported that the E_{corr} becomes nobler and the i_{corr} gets lower as the amount of P in the Ni-P alloy coatings increases [19], which implies that the Ni-P alloys with a high content of phosphorus

have a positive effect on anti-corrosion property of coatings [20-22].

Based on the above, this study aims to explore the influence of applied current density on the morphological, chemical composition and structural properties of Ni-P alloy coatings fabricated on pre-treated steel substrates by electrodeposition route from an economical bath. To determine the anti-corrosion capability of Ni-P alloys bombard corrosion attacks by Cl⁻ ions, the samples were examined in aggressive 1 M HCl media using both lost weight and potentiodynamic polarization technique.

2. EXPERIMENTAL PROCEDURES

2.1. Electrodeposition of Ni-P alloy coatings

The Ni-P coating was deposited on copper substrates from an economical bath containing NiSO₄·7H₂O, sodium hypophosphite (NaH₂PO₂·2H₂O), (NaCl), boric acid (Table.1). Bi-distilled water was used for the preparation of the electrolyte. The coatings were obtained by varying the current densities from (1 to 3A.dm⁻²). To assure the enrichments of the electrolyte by Nickel ions, tow nickel sheets of commercial purity (99.99%) were used as an anode. Copper substrates (99.9 %) were used as cathode.

Copper samples were processed in three steps, (1): mechanically polishing with SiC abrasive paper (120 – 4000) Track by rinsing with distilled water and kept in an acetone solution. (2): degreasing in a solution containing (50 g.l⁻¹ Na₂CO₃ and 15 g.l⁻¹ NaOH) to remove greases. (3): pickling in 10% HCl solution to remove oxide traces, and finally washing with bi-distilled water. The pH of the bath was adjusted by adding HCl or NaOH solution.

2.2. Characterization of Ni-P alloy coatings

In order to test the Ni-P alloy coatings adhesion on copper substrates, the samples were heated for 30 minutes at 250°C and then submerged in water at room temperature [23]. The morphology of Ni-

P coatings was examined by FEI QUANTA 200 scanning electron microscopy (SEM). The compositions of Ni-P alloy coatings were determined with energy dispersive x-ray spectroscopy (EDS) analysis tool attached to the SEM. To determine the structure and phases composition, the XRD analysis was performed by the Bruker x-ray diffractometer (D8 Advance model) with Cu K_α radiation (1.5406 Å). The mean grain size was determined from the width of the peak by the Scherrer equation modified by Warren and Biscoe (Eq.1) [24].

$$\tau = 0.94\lambda/\beta\cos\theta \quad (1)$$

Where: θ is the position of the peak in the diffractogram, β is the integral peak broadening (in radians) which is approximately the full width at half maximum (FWHM) value, λ is the wavelength (in Å), and τ is the grain size. For estimating the crystal size, an average value is considered to be FWHM (or β). Hardness measurements were performed by Wilson 402UD Wolpert instrument, according to the Vickers method, with an applied load of 50 N for 10 seconds. Mean value was taken for at least five measurements performed at different locations in each sample.

Corrosion experiments of Ni-P coating in 1M HCl solution was determined by methods. The first corrosion test was performed using lost weight method of the samples immersed in 1M HCl during 30 days. The submerged surface is estimated at 1.16 cm². The corrosion rate was calculated using (Eq. 2) [25].

$$T_{\text{corr}} = 365\Delta m/St \quad (2)$$

Where: T_{corr} is corrosion rate (g/cm².y), $\Delta m = m_1 - m_2$ (m_1 is the weight before immersion (g), m_2 is the weight after immersion (g)), S : surface of the immersed sample (cm²) and t is immersion period (year).

Potentiodynamic polarization measurements have been conducted by using a standard three-electrode cell with the Ni-P electrodes (1.16 cm²) as a working electrode, Pt as auxiliary electrode

Table 1. Chemical composition and Ni-P Coatings deposition parameters.

Electrolytes	Concentrations	Deposition conditions	
NiSO ₄ ·7H ₂ O	52 g/l	temperature	75 °C
NaH ₂ PO ₂ ·2 H ₂ O	26 g/l	Current density	1-3 A.dm ⁻²
H ₃ BO ₃	24 g/l	Deposition Time	30 min
NaCl	40 g/l	pH	3±1
C ₇ H ₅ NO ₃ S	0.1 g/l		

and saturated calomel electrode as a reference electrode, all have immersed 1 M HCl corrosion media. This cell is connected to Voltalab 20 (PGP201) device working at a scanning rate of 20 mV/s. Corrosion rate (mm/y), corrosion potential E_{corr} (mV) and Tafel slopes (mV/s) have been calculated by using Tafel fitting technique provided by Volta Master 4 software.

3. RESULTS & DISCUSSION

The adhesion tests for all the samples showed that Ni-P alloy coatings have a good adhesion to the substrates. SEM analysis results of Ni-P alloy coatings fabricated at different current densities

have been shown in (Fig.1). It is clear that the surface of Ni-P coatings is uniform with the presence of some cracks and surface gaps, especially those prepared at low current densities. This is due to the low overvoltage of phosphorus. Also, the grains are spherical and their distribution and uniformity on the surface increase with the increase in the current density. (Fig.2) shows the EDX and graphical images results of various developed deposits. The nickel element appears in green which represents the majority on the surface of the deposits, while phosphorous element appears in red where it can be seen its distribution on the grains.

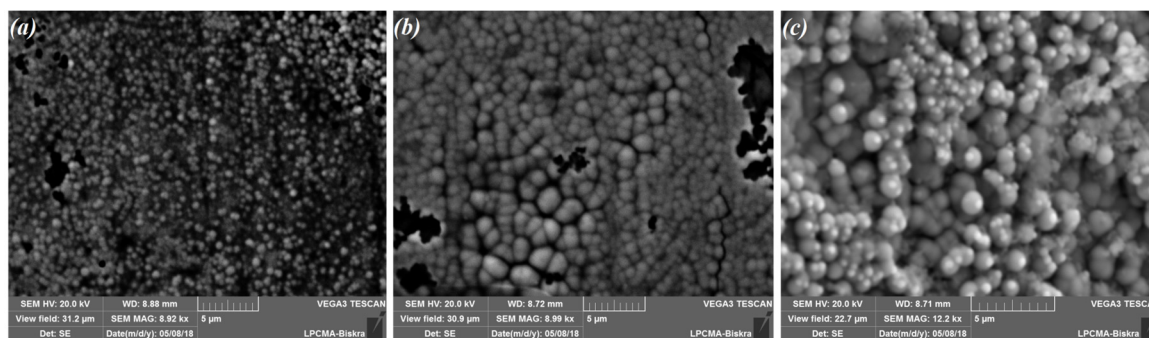


Fig. 1. SEM images of Ni-P coatings electrodeposited at : (a) 1 A.dm⁻²; (b) 2 A.dm⁻²; (c) 3 A/dm⁻².

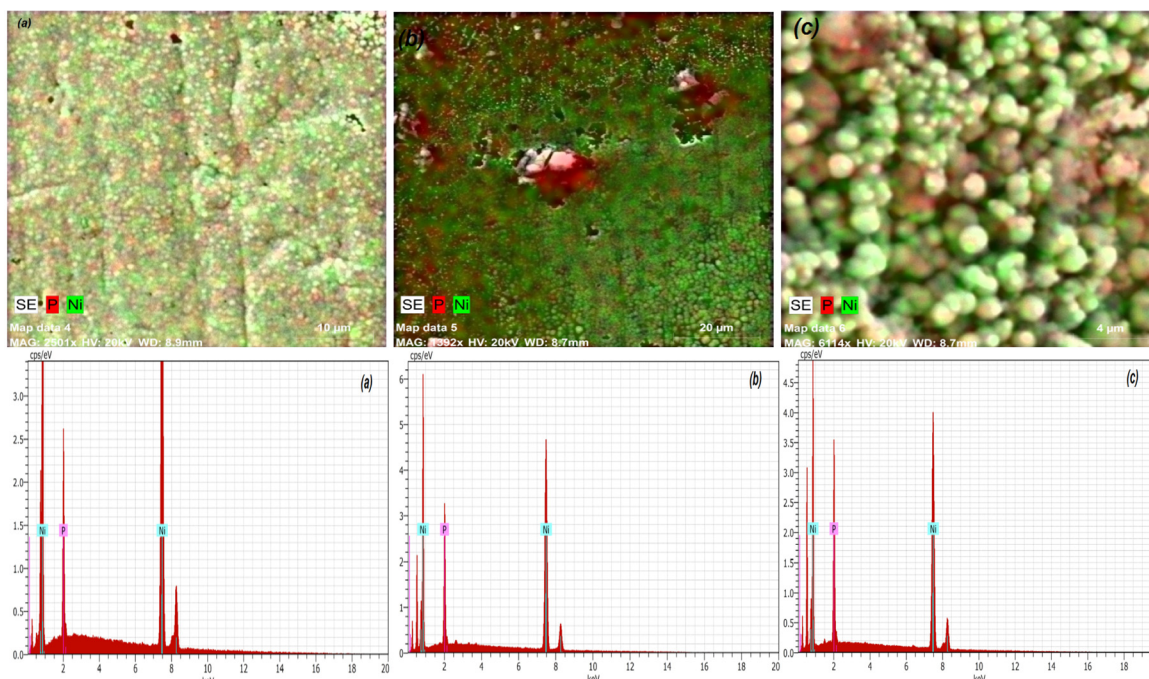


Fig. 2. Graphic images and EDX analysis of Ni-P alloy electrodeposited at various current densities: (a) 1 A.dm⁻²; (b) 2 A.dm⁻²; (c) 3 A.dm⁻².

This explains the appearance of a nickel-phosphorous mixture phase. (Fig.3) shows the chemical composition of the coating as a function of current density, the phosphorus content in the deposits increase with increasing applied current density and reaches the maximum value (18.37 wt%) at 3 A/dm² (Table 2). This evolution is due to the intensification of P ions reduction reaction.

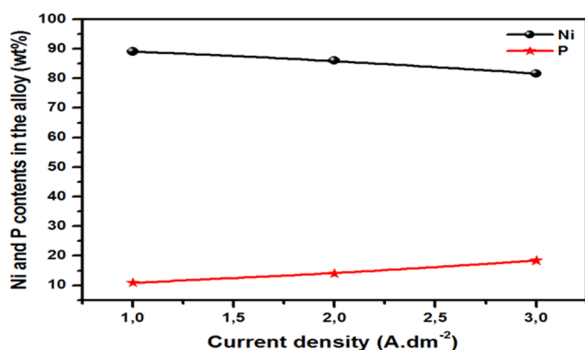


Fig. 3. Effect of applied current density on Ni and P content in the alloy coatings.

XRD analysis has been performed to determine the phase composition present in the developed coatings (Fig.4). It can be seen that no diffraction peaks of Cu are found in all patterns which implies that copper substrates are completely covered by Ni-P coatings.

At current density of 1 A/dm², XRD patterns show a single peak of NiP at 2θ=29.33° with (121)

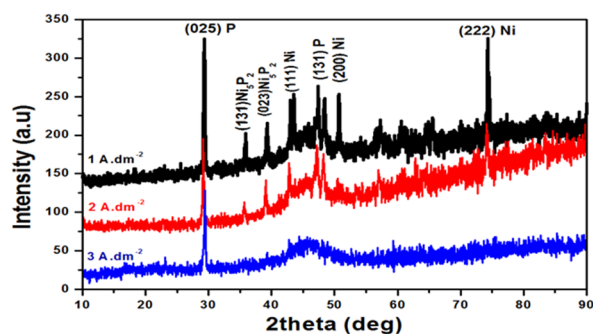


Fig. 4. XRD patterns of Ni-P alloys deposits as a function of applied current density.

orientation (orthorhombic structure, ASTM reference code: 00-018-0882), which is the common one for all the samples. This result is very consistent with the distribution of phosphorous color on all the spherical grains (Fig.2). The increase of current density led to the appearance of other peaks of NiP phase at 2θ=35.70° and 47.89° corresponding to the following orientation (112) and (220),

respectively. In addition, Ni phases appear at 2θ=39.49° (100) (hexagonal structure, ASTM reference code: 01-089-7129), also reveal at 2θ=43.27°, 50.58° and 74.42° with the orientation (111), (200) and (220), respectively, (hexagonal structure, ASTM reference code: 00-001-1260). The grains size and microhardness of Ni-P alloy coatings as a function of P content in the deposits are shown in (Fig. 5). It is clear that the increase in P content due to the increase of current density led to an increase of grains size values and decrease in the hardness of the deposits, which leads us to conclude that the P content in the deposits has a proportional relation with the grains size, and inverse relation with the hardness (Table.2). These results are due to the increase of the main peak intensity (Fig.4). To evaluate the protection capability of the Cu-coated Ni-P alloy coatings against corrosion attacks; the corrosion test has been carried out using lost weight method.

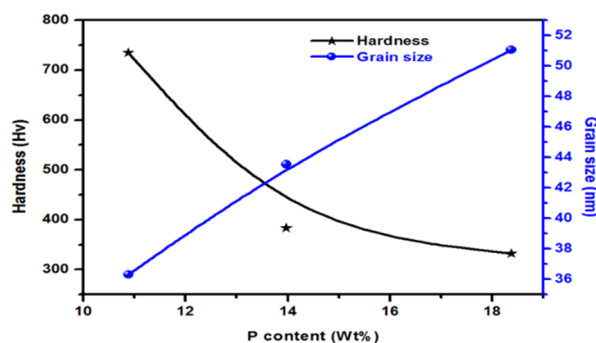


Fig. 5. Effect of P content in the deposits on the grains size and microhardness of Ni-P alloy coatings.

(Fig.6) shows the variation of corrosion rate with current density in corrosive media (1M HCl) for 30 days at room temperature. The corrosion rate increase with the increasing of applied current density and the P content.

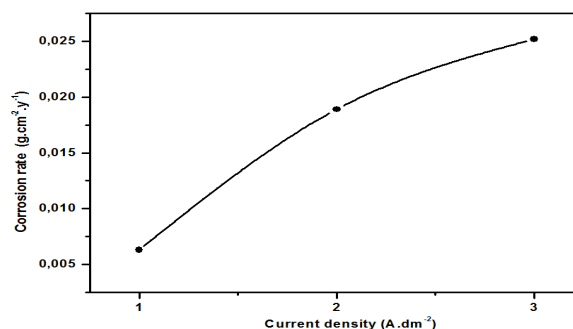


Fig. 6. Corrosion rate of Ni-P coatings as a function of applied current density.

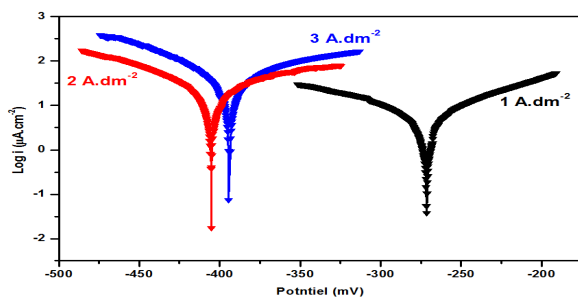
Table 2. the influence of P content on the grains size and the hardness of Ni-P deposits

Current density (A/dm ²)	P content (wt.%)	Grains size (nm)	Hrdness (Hv)
1	10.88	36.31	735
2	13.97	43.55	383.6
3	18.37	51.06	332.2

This is due to the increase in the grains size and its distribution on the entire surface which leads to the enhancement of surface contact between corrosion medium and Ni-P alloy coatings. Ralston and Birbilis [26] disclosed that grain refinement leads to improvements in strength and wear resistance.

Inherent processing involved in grain refinement alters both the bulk and the surface of a material, leading to changes in grain boundary density, orientation, and residual stress. Hence, improves the electrochemical behaviour and, consequently, corrosion susceptibility.

The polarization curves obtained for Ni-P coatings, in 1 M HCL solution, are shown in (Fig. 7). The corrosion potential (E_{corr}) and corrosion current density (i_{corr}) calculated using Tafel extrapolation method is given in (Table.2).

**Fig. 7.** Polarization curves of Ni-P alloy coatings electrodeposited at various current densities.

The corrosion resistance of Ni- (18.37 wt %) P coating is higher than that of the other two types of coatings, the E_{corr} becomes nobler (-271, 4 mV) and the i_{corr} gets lower (4, 64 $\mu\text{A}/\text{cm}^2$) as the

amount of P in the Ni-P alloy coatings decreases (Table.3), supporting the results of earlier study [27]. according to several published researches [28-29], It is known that the corrosion resistance increases with increasing P content in the deposits. Raicheff and Zaprianova [30] have reported that homogeneous structure and the absence of grain boundaries are responsible on the higher corrosion resistance of amorphous Ni-P coatings [28].

4. CONCLUSIONS

Ni-P alloy coatings were electrodeposited from sulfate baths to study the dependence of the morphology, chemical composition, structure, and mechanical properties at various current densities. Ni-P alloy coatings were strongly influenced by the electroplating current density. SEM images revealed spherical grains distributed uniformly on the surface. EDX study showed linear increase of P content in the deposits with the current intensity.

DRX patterns analysis showed that NiP phase with orthorhombic structure is the common peak in all samples. Moreover, its intensity enhanced with increasing current density. This led to an increase in the grains size and a decrease in the hardness values in the coatings.

Lost weight and potentiodynamique polarization studies revealed that the best values of E_{corr} (-271, 4 mV) and the lowest i_{corr} (4, 64 $\mu\text{A}/\text{cm}^2$) was observed in the coating with low P content prepared at 1 A/dm².

Table 3. Results of polarization measurements for Ni-P alloy coatings deposited at various current density in 1 M HCl.

Current density (A.dm ²)	E_{corr} (mV)	i_{corr} (mA.cm ⁻²)	R_p (ohm.cm ²)
1	-271.4	$4,64.10^{-3}$	2560
2	-405.3	$19,86.10^{-3}$	585,01
3	-394	$35,9.10^{-3}$	320,33

REFERENCES

- [1] Sknar, Y. E., Savchuk, O. O. and Sknar, I. V., "Characteristics of electrodeposition of Ni and Ni-P alloys from the sulfonate electrolyte." *Appl. Surf. Sci.*, 423, 2017, 340-348. Doi.org/10.1016/j.apsusc.2017.06.146.
- [2] Chang, L., Chen, C. H. and Fang, H., "Electrodeposition of Ni-P Alloys From a Sulfamate Electrolyte Relationship Between Bath pH and Structural Characteristics." *Journal of the Electrochemical Society*, 155, 2008, D57-D61. Doi: 10.1149/1.2803516.
- [3] Li, L., Zhang, Y., Deng, S. and Chen, Y., "Effect of ammonium on low temperature electrodeposition of Ni-P alloys." *Mater Lett.*, 57, 2003, 3444-8. Doi: 10.1016/S0167-577X(03)00097-1.
- [4] Mahalingam, T., Raja, M., Thanikaikarasan, S., Sanjeeviraja, C., Velumani, S., Moon, H. and Deak Kim, Y., "Electrochemical deposition and characterization of Ni-P alloy thin films." *Materials Characterization*, 58 (2007) 800-804. Doi:10.1016/j.matchar.2006.11.023.
- [5] Suzuki, Y., Arai, S. and Endo, M., "Electrodeposition of Ni-P Alloy-Multiwalled Carbon Nanotube Composite Films. *Journal of the Electrochemical Society*, 157, 2010, D50-D53. <https://doi.org/10.1149/1.3254180>.
- [6] Torre, F. D., Swygenhoven, H. V. and Victoria, M., "Nanocrystalline electrodeposited Ni: microstructure and tensile properties." *Acta Materialia*, 50, 2002, 957-970. DOI: 10.1016/S1359-6454(02)00198-2.
- [7] Ma, C., Wang, S. C., Wang, L.P., Walsh, F. C. and Wood, R. J. K., "The electrodeposition and characterisation of low-friction and wear-resistant Co-Ni-P coatings." *Surface and Coatings Technology*, 235, 2013, 495-505. <https://doi.org/10.1016/j.surfcoat.2013.08.009>.
- [8] He, Y., Wang, S. C., Walsh, F. C., Chiu, Y. L. and Reed, P. A. S., "Self-lubricating Ni-P-MoS₂ composite coatings." *Surface and Coatings Technology*, 307 (2016) 926-934. <https://doi.org/10.1016/j.surfcoat.2016.09.078>.
- [9] Saitou, M., Okudaira, Y. and Oshikawa, W., "Amorphous Structures and Kinetics of Phosphorous Incorporation in Electrodeposited Ni-P Thin Films." *Journal of The Electrochemical Society*, 150, 2003, C140-C143. <https://doi.org/10.1149/1.1545459>.
- [10] Daly, B. P. and Barry, F. J., "Electrochemical nickel phosphorus alloy formation." *Int. Mater. Rev.* 48, 2003, 326-338. <https://doi.org/10.1179/095066003225008482>.
- [11] Ng, P. K., Snyder, D. D., LaSala, J., Clemens, B. and Fuerst, C., Structure and crystallization of nickel phosphorus alloys prepared by high-rate electrodeposition. *J. Electrochem. Soc.*, 135, 1988, 1376-1381. <https://doi.org/10.1149/1.2095994>.
- [12] Balaraju, J. N., Sankara Narayanan, T. S. N. and Seshadri, S. K., "Electroless Ni-P composite coatings." *J. Appl. Electrochem.*, 33, 2003, 807-816. DOI: 10.1023/A:1025572410205.
- [13] Carbajal, J. L. and White, R. E., "Electrochemical Production and Corrosion Testing of Amorphous Ni-P." *J. Electrochem. Soc.*, 135, 1988, 2952-2957. Doi: 10.1149/1.2095468.
- [14] Brenner, A., *Electrodeposition of Alloys*, vol. 1, Academic Press, New York, 1963.
- [15] Zeller, R. L. and Landau, U., "Electrodeposition of Ni-P Amorphous Alloys." *J. Electrochem. Soc.*, 139, 1992, 3464-3469. Doi: 10.1149/1.2069100.
- [16] Morikawa, T., Nakade, T., Yokoi, M., Fukumoto, Y. and Iwakura, C., "Electrodeposition of Ni-P Alloys from Ni-Citrate Bath." *Electrochim. Acta.*, 42, 1997, 115-118. Doi:10.1016/0013-4686(96)00173-9.
- [17] Pillai, A. M., Rajendra, A. and Sharma, A. K., "Electrodeposited nickel-phosphorous (Ni-P) alloy coating: an in-depth study of its preparation, properties and structural transitions." *J. Coat. Technol. Res.*, 9, 2012, 785-797. Doi 10.1007/s11998-012-9411-0.
- [18] Murugan, V. K., Jia, Z., Syaranamual, G. J., Gan, C. L., Huang, Y. and Chen, Z., "An investigation into different nickel and nickel-phosphorus stacked thin coatings



- for the corrosion protection of electrical contacts." *Surf. Coat. Technol.*, 300, 2016, 95-103. Doi.10.1016 / j.surf coat. 2016.05.013.
- [19] You, Y., Gu, C., Wang, X. and Tu, J., "Electrochemical Synthesis and Characterization of Ni-P Alloy Coatings from Eutectic-Based Ionic Liquid." *Journal of The Electrochemical Society*, 159, 2012, D642-D648. <https://doi.org/10.1149/2.012211jes>.
- [20] Gu, C. D., Lian, J. G., Li, L. N. and Jiang, Z., "Electroless Ni-P plating on AZ91D magnesium alloy from a sulfate solution." *J. Alloy. Compd.*, 391, 2005, 104. <https://doi.org/10.1016/j.jallcom.2004.07.083>.
- [21] Gu, C. D., Lian, J. G., Li, L. N. and Jiang, Z., "High corrosion-resistant Ni-P/Ni/Ni-P multilayer coatings on steel." *Surf. Coat. Technol.*, 197, 2005, 61. <https://doi.org/10.1016/j.surfcoat.2004.11.004>.
- [22] Gu, C. D., Lian, J. G. and Jiang, Z., "Multilayer Ni-P Coating for Improving the Corrosion Resistance of AZ91D Magnesium Alloy." *Adv. Eng. Mater.*, 7, 2005, 1032. <https://doi.org/10.1002/adem.200500136>.
- [23] Ben Temam, H., Chala, A. and Rahmane, S., "Microhardness and corrosion behavior of Ni-SiC electrodeposited coatings in presence of organic additives." *Surface & Coatings Technology*, 205, 2011, S161-S164. [Doi.org/10.1016/j.surfcoat.2011.04.086](https://doi.org/10.1016/j.surfcoat.2011.04.086).
- [24] L Sanches, L. S., Domingues, S. H., Marino, C. E. and Mascaro, L. H., "Characterisation of electrochemically deposited Ni-Mo alloy coatings." *Electrochem. Commun.*, 6, 2004, 543-548. DOI:10.1016/j.elecom.2004.04.002.
- [25] Karayianni, H. S., Batis, G. and Vassiliou P., "Corrosion resistance of composite nickel-Al₂O₃ deposits." *Anti-Corrosion Methods and Materials*, 46, 2004, 29-34. [Doi.org/10.1108/00035599910252767](https://doi.org/10.1108/00035599910252767).
- [26] Ralston, K. D. and Birbilis, N., "Effect of Grain Size on Corrosion: A Review." *CORROSION*, 66, 2010, 075005-075005-13. <https://doi.org/10.5006/1.3462912>.
- [27] Hung, K. C., Chan, Y. C., Tang, C. W. and Ong, H. C., "Correlation between Ni₃Sn₄ intermetallics and Ni₃P due to solder reaction-assisted crystallization of electroless Ni-P metallization in advanced packages." *J. Mater. Res.*, 15, 2000, 2537. <https://doi.org/10.1557/JMR.2000.0363>.
- [28] Sankara Narayanan, T. S. N., Baskaran, I., Krishnaveni, K. and Parthiban, S., "Deposition of electroless Ni-P graded coatings and evaluation of their corrosion resistance." *Surface & Coatings Technology*, 200, 2006, 3438- 3445. <https://doi.org/10.1016/j.surfcoat.2004.10.014>.
- [29] Lu, G. and Zangari, G., "Corrosion resistance of ternary Ni-P based alloys in sulfuric acid solutions." *Electrochim. Acta.*, 47, 2002, 2969. DOI: 10.1016/S0013-4686(02)00198-6.
- [30] Jang, J. W., Kim, P. G., Tu, K. N., Frear, D. R. and Thompson, P., "Solder reaction-assisted crystallization of electroless Ni-P under bump metallization in low cost flip chip technology." *J. Appl. Phys.*, 85, 1999, 8456. <https://doi.org/10.1063/1.370627>.